The Journal of Chemical Physics

Parametrization of the Fe–O_{water} cross-interaction for a more accurate Fe_3O_4/water interface model and its application to a spherical Fe_3O_4 nanoparticle of realistic size

Cite as: J. Chem. Phys. **154**, 034702 (2021); https://doi.org/10.1063/5.0035678
Submitted: 30 October 2020 • Accepted: 23 December 2020 • Published Online: 15 January 2021

Paulo Siani, Enrico Bianchetti, Hongsheng Liu, et al.

The Journal of Chemical Physics ARTICLE scitation.org/journal/jcp

Parametrization of the Fe–O_{water} cross-interaction for a more accurate Fe_3O_4/water interface model and its application to a spherical Fe_3O_4 nanoparticle of realistic size

Cite as: J. Chem. Phys. 154, 034702 (2021); doi: 10.1063/5.0035678
Submitted: 30 October 2020 • Accepted: 23 December 2020 •
Published Online: 15 January 2021

Paulo Siani,[1] Enrico Bianchetti,[1] Hongsheng Liu,[1,2] and Cristiana Di Valentin[1,a)]

AFFILIATIONS

[1] Dipartimento di Scienza dei Materiali, Università di Milano-Bicocca, via R. Cozzi 55, 20125 Milano, Italy
[2] Laboratory of Materials Modification by Laser, Ion and Electron Beams, Dalian University of Technology, Ministry of Education, Dalian 116024, China

Note: This paper is part of the JCP Special Collection in Honor of Women in Chemical Physics and Physical Chemistry.
[a)] **Author to whom correspondence should be addressed:** cristiana.divalentin@unimib.it

ABSTRACT

The accurate description of iron oxides/water interfaces requires reliable force field parameters that can be developed through comparison with sophisticated quantum mechanical calculations. Here, a set of CLASS2 force field parameters is optimized to describe the Fe–O_{water} cross-interaction through comparison with hybrid density functional theory (HSE06) calculations of the potential energy function for a single water molecule adsorbed on the Fe_3O_4 (001) surface and with density functional tight binding (DFTB+U) molecular dynamics simulations for a water trilayer on the same surface. The performance of the new parameters is assessed through the analysis of the number density profile of a water bulk (12 nm) sandwiched between two magnetite slabs of large surface area. Their transferability is tested for water adsorption on the curved surface of a spherical Fe_3O_4 nanoparticle of realistic size (2.5 nm).

I. INTRODUCTION

Iron oxides/water interfaces are involved in many fundamental and technological processes, and therefore, accurate force field (FF) parameters for the description of the bond between surface iron sites and water oxygens, which we provide through this work, are critical to perform useful molecular dynamics simulations in this fast-developing research field.

Water adsorption on the low-index (001) Fe_3O_4 facet has been extensively investigated in the past through both experiments and theoretical calculations.[1–11] In particular, a mixed undissociated/dissociated adsorption mode was determined for one water monolayer adsorbed on the surface by means of a combined experimental and computational study.[11] On half of the metal adsorption sites, water molecules dissociate, forming a partially hydroxylated surface, whereas on the remaining adsorption sites, water adsorbs molecularly. In a previous work by our group,[12] we have investigated the behavior of water multilayers with increasing thickness up to 12 nm by comparing density functional tight binding (DFTB) results with molecular-mechanics molecular-dynamics simulations.

However, the classical model that we used,[12] although catching the general aspects of the water structure and solvation, has shown limited accuracy in the description of the details of the water coordination to the exposed surface undercoordinated iron sites. In the above-mentioned model, we observed longer distances (~2.7 Å to 2.8 Å) between the superficial iron atoms and the oxygen atoms of adsorbed water molecules (from now on, Fe–O_{water}) compared to higher-level calculations using hybrid DFT (density functional theory) and Hubbard corrected SCC-DFTB (self-consistent charge

density functional tight binding; from now on, DFTB+U) methods that predict Fe–O_{water} distances about 2.2 Å.

Herein, we provide an optimized set of CLASS2 force field parameters that corrects this issue and, therefore, accurately describes, at the classical level, the water coordination on the Fe sites over the partially hydroxylated Fe_3O_4(001) surface. In addition, we observe a quantitative agreement of surface and bulk properties between classical molecular-mechanics molecular-dynamics (from now on, classical MM-MD) simulations and DFTB+U molecular dynamics (from now on, DFTB-MD) simulations for a bulk-water density distribution along the Fe_3O_4(001) surface normal. Finally, we test the transferability of the optimized parameters for the description of the water adsorption on the curved surface of a spherical Fe_3O_4 nanoparticle [from now on, nanosphere (NS)] of realistic size with a diameter of 2.5 nm.

II. COMPUTATIONAL METHODS

All atomistic MM-MD simulations were carried out with the LAMMPS program (version 7 August 2019).[13] We made use of the CLASS2 potentials [see Ref. 14 for a full description of the COMPASS/CLASS2 force field (FF)]. This FF describes the non-bonded interactions for the repulsive and dispersive van der Waals forces through a Lennard-Jones 9-6 potential form [Eq. (1)], whereas the long-range electrostatic interactions are modeled by a classical Coulomb functional form [Eq. (2)],

$$E_{vdW} = \sum_{i,j} \epsilon_{ij} \left[2\left(\frac{\sigma_{ij}^0}{r_{ij}}\right)^9 - 3\left(\frac{\sigma_{ij}^0}{r_{ij}}\right)^6 \right], \tag{1}$$

$$E_{elec} = \frac{1}{4\pi\epsilon_0} \sum_{i,j} \frac{q_i q_j}{r_{ij}}. \tag{2}$$

Here, σ_{ij} defines the inter-atomic distance between a pair of atoms at which the potential energy function (PEF) assumes a minimum value and ε_{ij} defines the potential well depth for this pairwise potential. q_i and q_j are the partial atomic charges on the atoms i and j. Bonded and non-bonded parameters for the CLASS2-based three-site water model and the hydroxyl group are taken from the INTERFACE-FF.[15] The LJ(9-6) parameters for the Fe(II), Fe(III), and O(II) atom types were taken from Ref. 16, and the partial atomic charges for these atoms were derived from the DFT/HSE06 calculations. For unlike atom types, the sigma and epsilon cross-parameters are given by the sixth power combining rules[14] according to the following equations:

$$\sigma_{i,j} = \left[\frac{\left(\sigma_i^0\right)^6 + \left(\sigma_j^0\right)^6}{2} \right]^{\frac{1}{6}} f_1, \tag{3}$$

$$\epsilon_{i,j} = 2\sqrt{\epsilon_i \epsilon_j} \left[\frac{\left(\sigma_i^0 \sigma_j^0\right)^3}{\left(\sigma_i^0\right)^6 + \left(\sigma_j^0\right)^6} \right] f_2, \tag{4}$$

respectively. The scanning of both epsilon and sigma Fe–O_w cross-parameters consists of systematic variation in the f_1 [Eq. (3)] and f_2 [Eq. (4)] factors over their original values (the case in which f_1 and f_2 are equal to unity) until the error function reaches satisfactory agreement against the reference dataset. This protocol is in line with a previously published protocol by one of the authors,[17]

$$RMSE = \sqrt{\frac{\sum_{i=1}^{n} \left(X_{MM,i} - X_{QM,i}\right)^2}{n}}. \tag{5}$$

Values close to zero indicate good agreement, whereas deviations to larger values indicate more flawed agreement between the MM ($X_{MM,i}$) and the QM reference ($X_{QM,i}$) predictions for the peak maximum position in the number density profiles. To accurately determine the QM reference data in Eq. (5), we estimate, through a non-linear Gaussian fitting, the first, second, and third maxima peaks in the DFTB-MD density profiles. The atomic coordinates of the Fe, O, and H in the Fe_3O_4 slab and NS freeze at the DFTB+U-optimized geometry with the zeroing of the forces on these atoms at every MM-MD simulation step. To avoid spurious effects due to water evaporation at the trilayer/vacuum interphase in the MM-MD simulations, we included sufficient water molecules between the third water layer and the vacuum phase to keep the inner solvation layers stable on the surface. To solvate this system, we made use of the PACKMOL program[18] to randomly displace the water molecules on both sides of the hydroxylated Fe_3O_4 slab by a ~12 nm-thick water multilayer, whose images are periodically repeated along the z-direction. To get a better molecular packing than what is provided by PACKMOL, we carried out an energy minimization calculation, where we allowed to relax the water molecules sandwiched between the opposite sides of the Fe_3O_4 slab (fixed at the original DFTB atomic positions of Fe_3O_4 atoms) and the cell dimension along the z-direction. We applied a stress tensor at P = 1 atm for the virial component of the pressure (the non-kinetic portion) along the z-component of the simulation box with a threshold for forces of 1×10^{-5}. On the xy-plane parallel to the Fe_3O_4 slab, a standard energy minimization of the water molecules, through the conjugate gradient algorithm with a threshold for forces of 1×10^{-5}, was performed. After this relaxation, the bulk-water dimension along the z-direction slightly shrinks to ~0.9%. The final bulk-water density is 0.997 g/cm^3, in excellent agreement with the experimental estimation of water density at T = 300 K and P = 1 atm (0.996 g/cm^3). The equilibration phase was carried out for 10 ns in the isotherm–isobaric (NVT) ensemble until convergence of the bulk-water density at T = 300 K. The production phase explored 50 ns of the phase space in the NVT ensemble at T = 300 K. The long-range solver particle–particle particle–mesh[19] handled the electrostatic interactions with a real space cutoff of 10 Å and a threshold of 10^{-6} for the error tolerance in forces. For the short-range LJ (9-6) potential, we used a cutoff of 10 Å. Newton's equations of motion were solved using the velocity-Verlet integrator with a time step of 1.0 fs.

A. Potential energy function (PEF) calculations

Density functional theory calculations of a single water molecule adsorbed on the bare Fe_3O_4(001) surface were used as a first benchmark to tune the force field parameters. The system was allowed to ionically relax to a stable configuration. The adsorption of water oxygen (O_{water}) on top of a surface five-coordinated Fe

ion at the octahedral site was observed, in agreement with a previous study.[11] Therefore, DFT/HSE06 calculations were performed for 23 configurations of the water molecule at different distances from the surface Fe. For this purpose, the adsorbed water molecule has been rigidly shifted along the surface normal. The adsorption energies of these configurations were obtained by performing Self-Consistent Field (SCF) calculations without any ionic relaxation. Then, a distance-dependent (Fe–O_{water}) potential energy function (PEF) was built up.

B. Density profile calculations

For the second refinement of FF parameters, linear number density profiles (atoms/Å) were calculated to fit the MM-MD and DFTB-MD results in which only O atoms belonging to the molecular water were considered. First, we have divided the space along the z coordinate into equally sized bins (Δz) of thickness set at 0.1 Å. Then, the particle count for each bin was normalized by the total count of particles and their size.

C. DFT and DFTB computational details

To tune the force field parameters, hybrid density functional theory calculations (HSE06) were carried out using the CRYSTAL17 package.[20,21] In these calculations, the Kohn–Sham orbitals are expanded in Gaussian-type orbitals [the all-electron basis sets are H|511G(p1), O|8411G(d1), and Fe|86411G(d41) according to the scheme previously used for Fe_3O_4].[9,22] The convergence criterion of 0.023 eV/Å for forces was used during geometry optimization, and the convergence criterion for total energy was set at 10^{-6} Hartree for all the calculations. The k points generated by the Monkhorst–Pack scheme were chosen to be 3 × 3 × 1 since the total energy difference was found to be below 1 meV when compared with larger grids up to 6 × 6 × 1. According to a previous report,[23] the inclusion of the van der Waals correction (DFT+D2)[24] only slightly changes the adsorption energy of water on the Fe_3O_4(110) surface, so no van der Waals correction is included in this work.

To further refine the force field parameters, molecular dynamics simulations are performed using the SCC-DFTB method implemented in the DFTB+ package.[25] The SCC-DFTB is an approximated DFT-based method that is derived from the second-order expansion of the Kohn–Sham total energy in DFT with respect to the electron density fluctuations. The SCC-DFTB total energy can be defined as

$$E_{tot} = \sum_{i}^{occ} \varepsilon_i + \frac{1}{2}\sum_{\alpha,\beta}^{N} \gamma_{\alpha\beta}\Delta q_\alpha \Delta q_\beta + E_{rep}, \tag{6}$$

where the first term is the sum of the one-electron energies ε_i coming from the diagonalization of an approximated Hamiltonian matrix, Δq_α and Δq_β are the induced charges on the atoms α and β, respectively, and $\gamma_{\alpha\beta}$ is a Coulombic-like interaction potential. E_{rep} is a short-range pairwise repulsive potential. More details about the SCC-DFTB method can be found in Refs. 26–28. DFTB will be used as a shorthand for SCC-DFTB.

For the Fe–Fe and Fe–H interactions, we used the "trans3d-0-1" set of parameters, as reported previously.[29] For the O–O, H–O, and H–H interactions, we used the "mio-1-1" set of parameters.[30] For the Fe–O interactions, we used the Slater–Koster files fitted by us previously,[31] which can well reproduce the results for magnetite bulk and surfaces from HSE06 and PBE+U calculations. To properly deal with the strong correlation effects among Fe 3d electrons,[32] DFTB+U with an effective U-J value of 3.5 eV was adopted according to our previous work on magnetite.[9,12,22,31,33] The convergence criterion of 10^{-4} a.u. for forces was used during geometry optimization together with the conjugate gradient optimization algorithm. The convergence threshold on the self-consistent charge (SCC) procedure was set to be 10^{-5} a.u. for flat Fe_3O_4(001) surface calculations and 5×10^{-3} a.u. for Fe_3O_4 NS calculations. The k points generated by the Monkhorst–Pack scheme were chosen to be 6 × 6 × 1 for flat Fe_3O_4(001) surface calculations. We further checked that the structure for the adsorption of water molecules is not affected by the inclusion of the van der Waals correction (DFTB+D3).[34,35] Since the variations are within 0.1 Å, no correction will be presented in the following.

DFTB+U molecular dynamics were performed within the canonical ensemble (NVT) using an Andersen thermostat to keep the temperature constant at 300 K. The total simulation time is 50 ps with a time step of 1 fs. The convergence threshold on the self-consistent charge (SCC) procedure was set to be 5×10^{-3} a.u., and the k points generated by the Monkhorst–Pack scheme were chosen to be 4 × 4 × 1 (since the total energy difference was found to be below 1 meV when compared with larger grids up to 6 × 6 × 1). To well describe the hydrogen bonds, a modified hydrogen bonding damping (HBD) function was introduced with a ζ = 4 parameter.[36]

For the Fe_3O_4(001) surface, we use the SCV model. According to previous reports, this structural model is more stable than other models.[37] We used the same structure presented in our previous works,[9,12,31] which is a (1 × 1) 17-layer slab with inversion symmetry. In the z-direction, a vacuum of more than 12 Å was introduced to avoid the spurious interaction between the periodic sides of the slabs. Five layers in the middle of the slab are kept fixed to the bulk positions, whereas the other layers are fully relaxed. For water adsorption, molecules were put on both sides of the slab. For the Fe_3O_4 NS, we use the model (with about 1000 atoms) proposed in our previous work.[33]

To evaluate the stability of one water molecule adsorbed on the Fe_3O_4(001) surface and the Fe_3O_4 NS, the adsorption energy (E_{ads}) was calculated as follows:

$$E_{ads} = \left(E_{total} - E_{slab/NS} - E_{H_2O}\right), \tag{7}$$

where E_{total} is the total energy of the whole system (surface slab/NS and adsorbed water), $E_{slab/NS}$ is the energy of the Fe_3O_4(001) surface slab or the energy of the Fe_3O_4 NS, and E_{H_2O} is the energy of one isolated water molecule.

III. RESULTS AND DISCUSSION

A. Fitting of potential energy function (PEF) from hybrid DFT(HSE06) calculations for one water molecule adsorbed on Fe_3O_4(001) surface

As stated earlier, by merely applying the sixth-power combining rules to describe the cross-interaction between this pair

of unlike atoms [see Eqs. (3) and (4)], the original sets of CLASS2-FF parameters, adopted in Ref. 11, led to an overestimated Fe–O_{water} distance. To tackle this issue, we carry out a systematic *ad hoc* parametrization of both the repulsive (step 1) and attractive (step 2) components in the Lennard-Jones (9-6) [from now on, LJ; see Eq. (1) in Sec. II] potential for this pair of unlike atoms. This procedure consists of an iterative two-step optimization (see the supplementary material for more details regarding the parametrization protocol): (1) estimation of the potential energy function (from now on, PEF) for the adsorption of a single water molecule on the bare Fe_3O_4(001) surface, seeking the best agreement between the hybrid DFT (HSE06) and the classical results and (2) fine-tuning of the epsilon cross-parameters (ε[Fe–O_{water}]) in a systematic fashion to find the best match between classical MM-MD and DFTB-MD predictions for the water–trilayer density profile. We construct an objective error function [Eq. (5) in Sec. II] to measure agreement between the QM (quantum mechanics) reference dataset and the corresponding classical MM-MD results.

Steps 1 and 2 are repeated until satisfactory agreement between the classical MM-MD and the DFTB-MD predictions is obtained. Since the accuracy of the latter method has been already validated against hybrid DFT calculations in our previous publication,[11] we use DFTB-MD results as the reference dataset for the water density profile. Moreover, such a large number of atoms is unpractical for standard higher-level calculations (e.g., *ab initio* DFT-MD simulations). It is also important to mention that partial atomic charges on the classical atoms are derived based on the DFT level of theory and are kept fixed during the entire optimization procedure (see Table S3 of the supplementary material).

Figure 1 shows the PEF for the adsorption of a single water molecule on the bare Fe_3O_4(001) surface. Starting from the DFT(HSE06)-optimized structure, the water molecule is rigidly shifted along the normal to the surface. To fit the target QM data, we carry out systematic scanning by employing multiplicative factors over the original set of CLASS2-FF parameters (brown curve), taken by us as starting-point in this optimization procedure. More details can be found in the supplementary material.

We first fine-tune the sigma cross-parameter [with the epsilon parameter given by Eq. (4)] to determine the best fit for the interatomic distance between the Fe–O_{water} pair of atoms. Once a good match for the position of the PEF minimum by QM and by MM is observed (Fig. 1), we fine-tune only the epsilon cross-parameter to adjust the well depth to the classical LJ potential.

B. Comparing MM-MD density profile with DFTB-MD calculations for a water trilayer on Fe_3O_4(001) surface

To assess the performance of this prime set of CLASS2-FF parameters obtained from the fitting of the DFT adsorption PEF (step 1), we carried out classical MM-MD simulations for the trilayer model system. We still observe unsatisfactory agreement between the classical MM-MD predictions and the DFTB-MD target data for the water-trilayer density profile along the Fe_3O_4(001) surface normal (item B of Fig. S1). Although it shows a definite improvement over that obtained by the original CLASS2-FF parameters in our previous publication,[11] we decide to carry out a further step of refinement to enhance agreement between the classical MM-MD results and the DFTB-MD reference dataset. In this second-step parametrization, we carry out a fine-tuning of the epsilon cross-parameter between the Fe and O_{water} atoms.

Figure 2 shows the water density profiles along the Fe_3O_4(001) surface normal. Classical MM-MD predictions using the final parametrized set of CLASS2-FF parameters are shown in cyan (trilayer model) and green (bulk-water model). The reference data

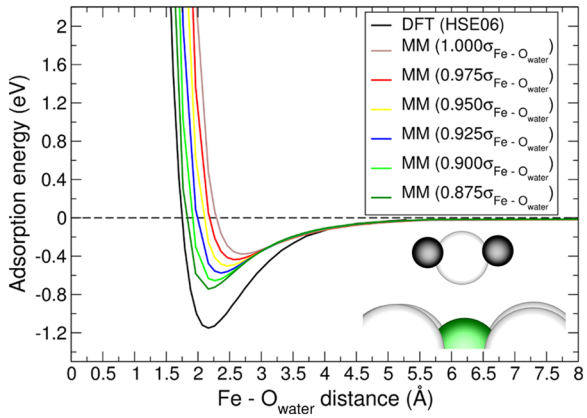

FIG. 1. PEFs for the adsorption of a single water molecule on the bare Fe_3O_4 (001) surface calculated at the DFT(HSE06) and the classical level of theory. The DFT curve is shown in black. All other colors represent each set of CLASS2 parameters and their respective profiles obtained by scanning up the cross-parameter epsilon and sigma between the Fe–O_{water} atoms. The inset shows the side view of the single water molecule adsorbed on the surface. The green, black, and small and large white beads represent Fe, H, and O from water and O from the surface, respectively.

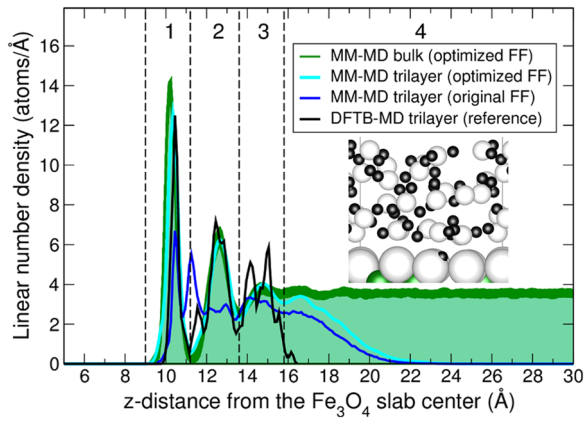

FIG. 2. Number density profiles of water molecules along the partially hydroxylated Fe_3O_4 (001) surface normal. DFTB-MD simulation (black), classical MM-MD bulk-water simulation (thick green line), classical MM-MD trilayer simulation with the optimized CLASS2-FF (cyan), and classical MM-MD trilayer simulation with the original CLASS2-FF (blue). Numbers between the dashed lines stand for different hydration shells. The inset shows the DFTB-MD water-trilayer model. The green, black, and small and large white beads represent Fe, H, and O from water and O from the surface, respectively.

for the water density profile predicted by the DFTB-MD simulations are shown in black. For the sake of comparison, we also include the water density profile estimated by the original model (blue) for the trilayer model in our previous publication.[12] The first two peaks for the MM-MD simulation with the original CLASS2-FF parameters merge into one single peak just above 10 Å for the simulation with the optimized parameters, in agreement with DFTB-MD results, thanks to the improved description of the Fe–O_{water} cross-interaction.

C. MM-MD density profile for bulk water on Fe_3O_4(001) surface

To further assess the performance of this final set of CLASS2-FF parameters (see Table S3 of the supplementary material), we built up a Fe_3O_4(001)/water interface model of realistic scale and density [bulk-water phase above and below the partially hydroxylated Fe_3O_4(001) slab of 80 × 80 $Å^2$ used for the trilayer model]. We then check whether the presence of bulk water could somehow affect the density of water molecules along the Fe_3O_4 (001) surface normal compared with the trilayer model. There are no substantial differences between the Fe_3O_4/trilayer-water (Fig. 2, cyan) and the Fe_3O_4/bulk-water (Fig. 2, green) MM-MD predictions for the water density profile, although a slight shift toward the surface is observed in the latter model.

Furthermore, we simulate an even larger model (160 × 160 $Å^2$) of a partially hydroxylated Fe_3O_4 surface containing a total of 112 624 water molecules. To the best of our knowledge, this system size is beyond any previous classical MM-MD simulation for the Fe_3O_4(001) surface/water interface to date. We notice that the most prominent finite-size effect is an induced ordering, mainly in the first solvation layer, as a consequence of the enlargement of the Fe_3O_4 surface area. This is evident in Fig. S2 of the supplementary material, where we observe a higher peak intensity for the Fe_3O_4 160 × 160 $Å^2$ surface (orange profile). Moreover, we observe no substantial difference in the farther solvation layers in the bulk water above the Fe_3O_4 surfaces.

D. Assessment of optimized FF parameters on single water molecule adsorption on Fe_3O_4(001) surface

The results above indicate that a Fe_3O_4 surface/water interface model, having both the realistic system size and bulk-water density, could take advantage of these new CLASS2-FF parameters. To corroborate this last assumption, we finally compare structural parameters of the optimized geometry of one water molecule adsorbed on bare and partially hydroxylated Fe_3O_4(001) surfaces at different levels of theory [see Figs. 3(a) and 3(b), respectively]. Table I shows that the interatomic distances from the optimized set of MM parameters are in better agreement with DFTB and DFT results compared to the original set. In particular, for the bare surface, the Fe–O_{water} distance was 2.84 Å with the original FF, which is quite too long with respect the DFT(HSE06) reference value of 2.16 Å, as we pointed out in our previous work,[11] whereas the same distance becomes 2.01 Å with optimized FF set of parameters, which is only 6.9% shorter than the reference value. Table S2 of the supplementary material shows that the adsorption energy obtained from the optimized set of FF parameters is in better agreement with DFTB and DFT data compared to the original FF. For instance, we observe an adsorption energy of −0.66 eV using the

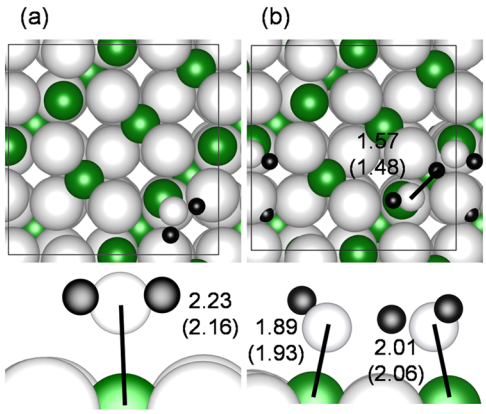

FIG. 3. Top and side views of a single water molecule adsorbed on (a) the bare Fe_3O_4(001) surface and (b) the partially hydroxylated Fe_3O_4(001) surface. The green, black, and small and large white beads represent Fe, H, and O from water and O from the surface, respectively. The hydrogen and Fe–O_{water} bonds are indicated by the solid lines. The bond length calculated by DFTB+U (outside the parantheses) and DFT/HSE06 (inside the parantheses) is given for each configuration. The black squares represent the ($\sqrt{2}$ × $\sqrt{2}$) R45° unit cell used in the calculations.

TABLE I. Structural parameters of one water molecule adsorbed on bare and partially hydroxylated Fe_3O_4 (001) surfaces. The inter-atomic distance obtained by using the DFT/HSE06 method is taken as the reference for calculating the error.

Inter-atomic distance (Å)	DFTB+U	DFT/HSE06	MM (original)	MM (optimized)
Fe–OH_2[a]	2.23	2.16	2.84 (31.5%)	2.01 (−6.9%)
Fe–OH[b]	1.89	1.93	1.89[c]	1.89[c]
Fe–OH_2[b]	2.01	2.06	2.69 (30.6%)	1.95 (−5.3%)
HO–HOH[b]	1.57	1.48	1.62 (9.5%)	1.54 (4.1%)
HO–OH_2[b]	2.57	2.52	2.60 (3.2%)	2.53 (0.4%)

[a]Bare surface [see Fig. 3(a)].
[b]Partially hydroxylated surface [see Fig. 3(b)].
[c]Fixed atoms in the slab.

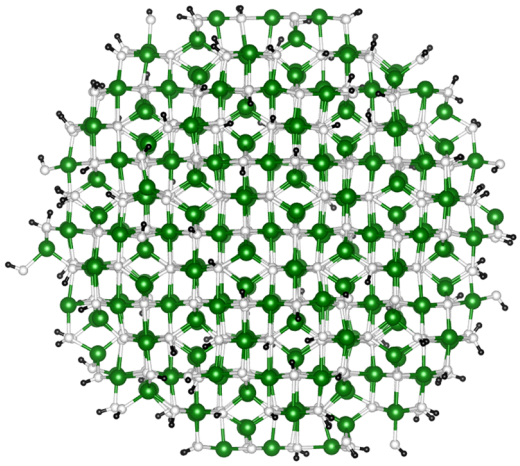

FIG. 4. Partially hydroxylated spherical Fe_3O_4 nanoparticle model of about 1000 atoms with a diameter of 2.5 nm. The green, black, and white beads represent Fe, H, and O, respectively.

original set of FF parameters, which is 43% of the DFT(HSE06) reference data of −1.15 eV, while the adsorption energy predicted by the optimized FF matches exactly the DFT(HSE06) reference value.

E. Assessment of the force fields for their use with spherical Fe_3O_4 nanoparticles

In this section, we present the assessment of the transferability of the newly optimized set of parameters for the description of water adsorption on a Fe_3O_4 NS of realistic size with about 1000 atoms (see Fig. 4).

To this end, we compare the adsorption structure and energy of a single water molecule on different sites of the partially hydroxylated Fe_3O_4 NS, as obtained at the MM level of theory with the CLASS2 force field parameters with the results from a quantum mechanical QM method. We use DFTB+U results as the QM reference dataset, since DFTB+U was previously validated against higher-level DFT results.[12] The MM results are obtained both through the direct optimization of DFTB+U structures (second rows of Tables II and III) and through the final optimization after 50 ns of the MM-MD simulation at 300 K (third rows of Tables II and III). In all the MM calculations, the structure of the partially hydroxylated Fe_3O_4 NS is kept fixed at the DFTB+U optimized geometry before water adsorption.

TABLE III. Binding energies (eV) of one water molecule adsorbed on different sites of a partially hydroxylated Fe_3O_4 NS at DFTB+U and MM levels of theory.

$E_{binding}$ (eV)	Site 1	Site 2	Site 3	Site 4	Site 5
DFTB+U	−1.03	−2.71	−1.35	−1.93	−1.54
MM (from DFTB+U)	−1.14	−1.97	−0.80	−2.00	−1.92
MM (from MM-MD)	...	...	...	−2.59	−2.78

When one water molecule is adsorbed on sites 1, 2, and 3 (see Fig. 5), MM structural results, when optimized both before and after molecular dynamics, very much resemble the DFTB ones. For the adsorption on sites 4 and 5, classical MM results before the MM-MD are in good agreement with those of DFTB ones [see Figs. 6(a) and 6(c)], while classical MM results after MD are slightly different [see Figs. 6(b) and 6(d)]. Figures 6(a) and 6(c) show that before the MM-MD simulations, the water molecule tends to form one hydrogen bond, whereas Figs. 6(b) and 6(d) show that after the MM-MD simulations, the water molecule interacts with two O atoms on the NS forming two H-bonds.

Table III reports the water binding energy values. We observe good agreement of the binding energies at DFTB+U and MM levels of theory. We also observe that the optimized configuration after the MM-MD simulation (third row) is more stable than the one optimized before the MM-MD (second row). We may notice that, due to the formation of a second H-bond after MM-MD, the water molecule undergoes a structural rearrangement. The Fe–O_{water} distance is not much affected, whereas the molecule rotates to allow the formation of the new H-bonds, resulting in a significantly reduced distance between the O_{water} atom and the NS centroid [see the second and third rows in Table II].

According to this assessment analysis, the transferability of the optimized CLASS2 set of FF parameters turns out to be less accurate as the Fe neighborhood becomes less similar to that of the Fe_3O_4(001) flat surface for which the parameters have been optimized. The MM-MD simulations, depending on the site morphology, tend to maximize the number of H-bonds established by the water molecule with the nanoparticle surface atoms, as discussed above. We do not observe this phenomenon in the classical Fe_3O_4(001) flat surface model because of the lower availability of neighboring surface O atoms as H-bond acceptors, as evident in Fig. 7(a). In particular, Fig. 7(a) shows that the adsorption site on

TABLE II. Fe–O_{water} inter-atomic distance (Å) of one water molecule adsorbed on different sites of a partially hydroxylated Fe_3O_4 NS at DFTB+U and MM levels of theory. The distance between the water oxygen atom and the center of the NS is given in parentheses.

Fe–OH_2 (Å)	Site 1	Site 2	Site 3	Site 4	Site 5
DFTB+U	2.09 (15.06)	1.94 (15.05)	2.02 (13.83)	1.99 (13.41)	2.01 (13.29)
MM (from DFTB+U)	2.08 (15.02)	1.94 (15.01)	2.04 (13.82)	1.99 (13.41)	1.94 (13.31)
MM (from MM-MD)	...	...	...	2.10 (13.05)	2.07 (13.01)

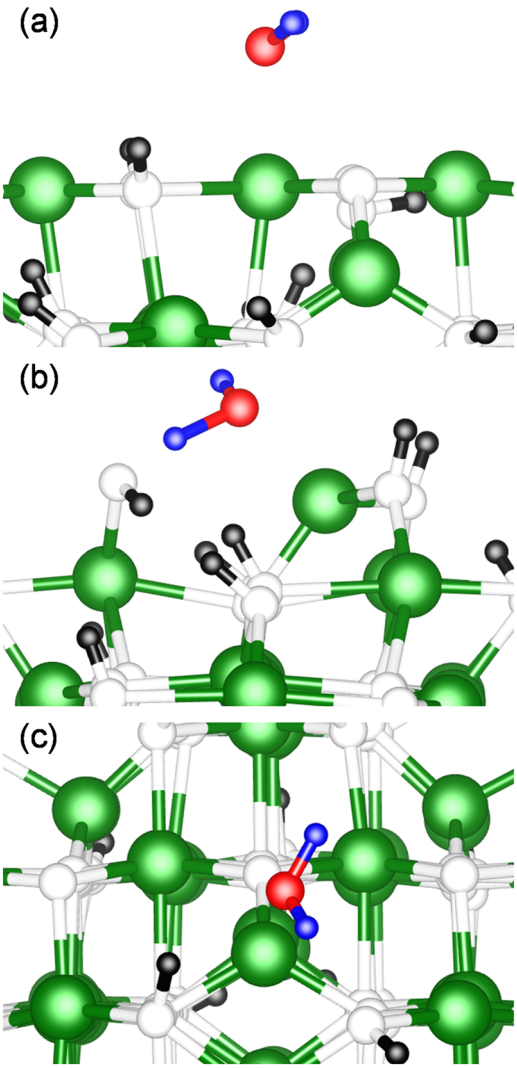

FIG. 5. Adsorption of one water molecule on (a) site 1, (b) site 2, and (c) site 3 at the DFTB+U level. Structures optimized at the MM level starting from DFTB+U ones are found to be nearly identical and are not reported. The green, black, white, blue, and red beads represent Fe, H, and O from the partially hydroxylated NS and H and O from the water molecule, respectively.

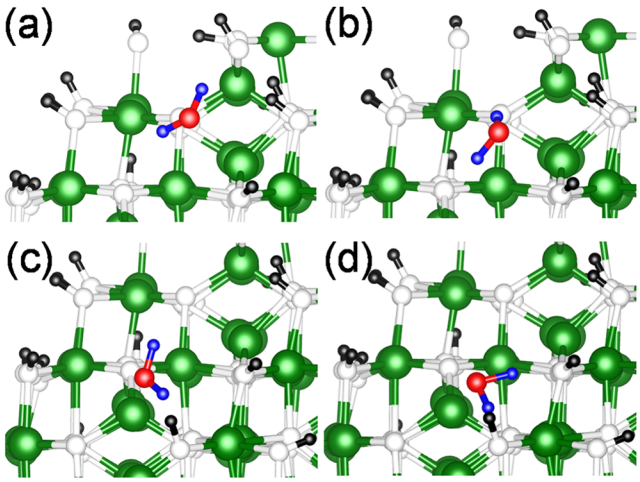

FIG. 6. Adsorption of one water molecule on site 4 [(a) and (b)] and site 5 [(c) and (d)] at the DFTB+U level of theory on the left and at the MM (optimized geometry after MM-MD) level of theory on the right. Structures optimized at the MM level starting from DFTB+U ones are nearly identical and not reported. The green, black, white, blue, and red beads represent Fe, H, and O from the partially hydroxylated NS and H and O from the water molecule, respectively.

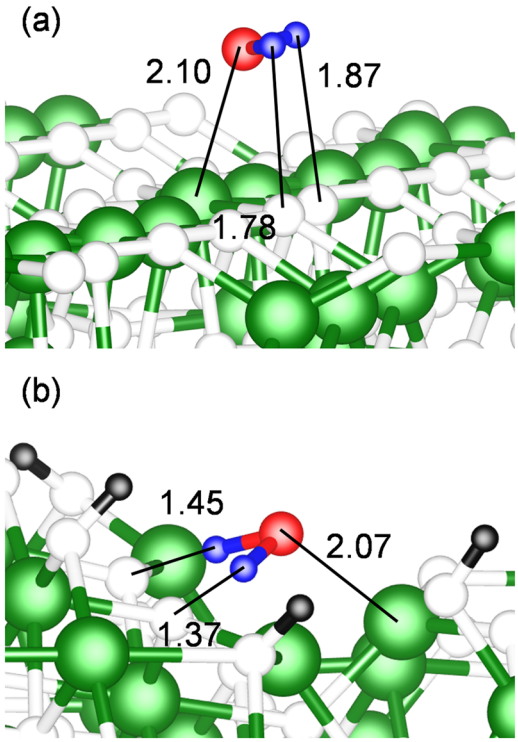

FIG. 7. Adsorption of one water molecule on (a) the Fe_3O_4 (001) surface and (b) site 5 of the partially hydroxylated Fe_3O_4 NS at the MM level of theory. Bonds are indicated by the black solid lines. The green, black, white, blue, and red beads represent Fe, H, and O from the partially hydroxylated NS and H and O from the water molecule, respectively.

the Fe_3O_4(001) flat surface is morphologically similar to the adsorption sites 1, 2, and 3 of the spherical nanoparticle in Fig. 5. On the contrary, the morphology of site 5 in Figs. 6(c) and 6(d), as in the case of site 4 in Figs. 6(a) and 6(b), is different from that of the flat surface. Here, several surface O atoms are available as H-bond acceptors and the water molecule can thus establish strong H-bonds (with an O–H–O angle of ~170° close to the optimal one of 180°).

We wish to add that for all the DFTB+U calculations, we made use of the HBD correction to get the best possible description of the H-bond interactions.[36] Based on the results above, we

conclude that the classical model tends to overestimate the H-bond interaction between the water molecule and the nanoparticle surface.

To conclude this section, based on the results presented and discussed above, we consider that the optimized set of CLASS2-FF parameters obtained in Sec. III A is suitable for the description of the water interface with a spherical Fe_3O_4 nanoparticle because they perform very well, with respect to the QM reference, in the description of the water adsorption on the surface of the spherical nanoparticle, especially when the adsorption site is morphologically similar to that of the flat (001) surface. They are still satisfactorily accurate, even when the adsorption site is more affected by the curvature, except for a rigid shift of the water O atom toward the center of the nanoparticle due to a molecular rotation to achieve the highest number of H-bonds with the surface, keeping the $Fe–O_{water}$ distance essentially unmodified.

IV. CONCLUSIONS

In the present work, we make available a new set of CLASS2-FF parameters (see the supplementary material) that accurately describe the molecular interaction between a partially hydroxylated Fe_3O_4 (001) surface and the interfacial/bulk-water molecules. Further development toward a combination of both the present CLASS2-FF parameters and the well-established CLASS2-FF parameters for Fe_3O_4/organic interfaces[12] opens up many possibilities on modeling and simulation of more complex Fe_3O_4/organic/water interfaces at realistic time and length scales. Here, we have proved their satisfactory transferability to the description of water adsorption on the curved surface of a spherical Fe_3O_4 nanoparticle of realistic size (2.5 nm).

SUPPLEMENTARY MATERIAL

See the supplementary material for further details regarding the parametrization protocol, the optimized LJ-parameters for the $Fe–O_{water}$ cross-interaction together with partial atomic charges for magnetite atoms, and the linear number density profile for the (160×160) Å^2 Fe_3O_4/bulk-water system.

DEDICATION

This paper is dedicated, on the occasion of her 70th birthday, to Professor Annabella Selloni, who performed groundbreaking work on the theoretical simulation of semiconducting oxides.

ACKNOWLEDGMENTS

The authors are grateful to Federico Soria for useful discussions and Lorenzo Ferraro for his technical help. This project received funding from the European Research Council (ERC) under the European Union's Horizon 2020 research and innovation programme (ERC Grant Agreement No. 647020).

DATA AVAILABILITY

The data that support the findings of this study are available from the corresponding author upon reasonable request.

REFERENCES

[1]C. H. F. Peden, G. S. Herman, I. Z. Ismagilov, B. D. Kay, M. A. Henderson, Y.-J. Kim, and S. A. Chambers, Catal. Today **51**, 513 (1999).
[2]T. Kendelewicz, P. Liu, C. S. Doyle, G. E. Brown, Jr., E. J. Nelson, and S. A. Chambers, Surf. Sci. **453**, 32 (2000).
[3]T. Kendelewicz, S. Kaya, J. T. Newberg, H. Bluhm, N. Mulakaluri, W. Moritz, M. Scheffler, A. Nilsson, R. Pentcheva, and G. E. Brown, J. Phys. Chem. C **117**, 2719 (2013).
[4]G. S. Parkinson, Z. Novotný, P. Jacobson, M. Schmid, and U. Diebold, J. Am. Chem. Soc. **133**, 12650 (2011).
[5]N. Mulakaluri, R. Pentcheva, M. Wieland, W. Moritz, and M. Scheffler, Phys. Rev. Lett. **103**, 176102 (2009).
[6]S. Liu, S. Wang, W. Li, J. Guo, and Q. Guo, J. Phys. Chem. C **117**, 14070 (2013).
[7]J. R. Rustad, A. R. Felmy, and E. J. Bylaska, Geochim. Cosmochim. Acta **67**, 1001 (2003).
[8]N. Mulakaluri, R. Pentcheva, and M. Scheffler, J. Phys. Chem. C **114**, 11148 (2010).
[9]G. S. Parkinson, Surf. Sci. Rep. **71**, 272 (2016).
[10]H. Liu and C. Di Valentin, Nanoscale **10**, 11021 (2018).
[11]M. Meier, J. Hulva, Z. Jakub, J. Pavelec, M. Setvin, R. Bliem, M. Schmid, U. Diebold, C. Franchini, and G. S. Parkinson, Proc. Natl. Acad. Sci. U. S. A. **115**, E5642 (2018).
[12]H. Liu, E. Bianchetti, P. Siani, and C. Di Valentin, J. Chem. Phys. **152**, 124711 (2020).
[13]S. Plimpton, J. Comput. Phys. **117**, 1 (1995).
[14]H. Sun, J. Phys. Chem. B **102**, 7338 (1998).
[15]H. Heinz, T.-J. Lin, R. Kishore Mishra, and F. S. Emami, Langmuir **29**, 1754 (2013).
[16]L. Zhao, L. Liu, and H. Sun, J. Phys. Chem. C **111**, 10610 (2007).
[17]P. Siani, H. Khandelia, M. Orsi, and L. G. Dias, J. Comput.-Aided Mol. Des. **32**, 1259 (2018).
[18]L. Martínez, R. Andrade, E. G. Birgin, and J. M. Martínez, J. Comput. Chem. **30**, 2157 (2009).
[19]R. W. Hockney and J. W. Eastwood, *Computer Simulation Using Particles* (CRC Press, Taylor & Francis Group, New York, 1989).
[20]R. Dovesi, A. Erba, R. Orlando, C. M. Zicovich-Wilson, B. Civalleri, L. Maschio, M. Rérat, S. Casassa, J. Baima, S. Salustro, and B. Kirtman, Wiley Interdiscip. Rev.: Comput. Mol. Sci. **8**, e1360 (2018).
[21]R. Dovesi, V. R. Saunders, C. Roetti, R. Orlando, C. M. Zicovich-Wilson, F. Pascale, B. Civalleri, K. Doll, N. M. Harrison, I. J. Bush, P. D'Arco, M. Llunell, M. Causà, Y. Noël, L. Maschio, A. Erba, M. Rerat, and S. Casassa, *CRYSTAL17 User's Manual* (University of Torino, Torino, 2017).
[22]H. Liu and C. Di Valentin, J. Phys. Chem. C **121**, 25736 (2017).
[23]U. Aschauer and A. Selloni, J. Chem. Phys. **143**, 044705 (2015).
[24]S. Grimme, J. Comput. Chem. **27**, 1787 (2006).
[25]B. Aradi, B. Hourahine, and T. Frauenheim, J. Phys. Chem. A **111**, 5678 (2007).
[26]W. M. C. Foulkes and R. Haydock, Phys. Rev. B **39**, 12520 (1989).
[27]G. Seifert and J.-O. Joswig, Wiley Interdiscip. Rev.: Comput. Mol. Sci. **2**, 456 (2012).
[28]M. Elstner and G. Seifert, Philos. Trans. R. Soc., A **372**, 20120483 (2014).
[29]G. Zheng, H. A. Witek, P. Bobadova-Parvanova, S. Irle, D. G. Musaev, R. Prabhakar, K. Morokuma, M. Lundberg, M. Elstner, C. Köhler, and T. Frauenheim, J. Chem. Theory Comput. **3**, 1349 (2007).
[30]M. Elstner, D. Porezag, G. Jungnickel, J. Elsner, M. Haugk, T. Frauenheim, S. Suhai, and G. Seifert, Phys. Rev. B **58**, 7260 (1998).

[31] H. Liu, G. Seifert, and C. Di Valentin, J. Chem. Phys. **150**, 094703 (2019).
[32] B. Hourahine, S. Sanna, B. Aradi, C. Köhler, T. Niehaus, and T. Frauenheim, J. Phys. Chem. A **111**, 5671 (2007).
[33] H. Liu and C. Di Valentin, Phys. Rev. Lett. **123**, 186101 (2019).
[34] S. Grimme, J. Antony, S. Ehrlich, and H. Krieg, J. Chem. Phys. **132**, 154104 (2010).
[35] S. Grimme, S. Ehrlich, and L. Goerigk, J. Comput. Chem. **32**, 1456 (2011).
[36] H. Hu, Z. Lu, M. Elstner, J. Hermans, and W. Yang, J. Phys. Chem. A **111**, 5685 (2007).
[37] R. Bliem, E. McDermott, P. Ferstl, M. Setvin, O. Gamba, J. Pavelec, M. A. Schneider, M. Schmid, U. Diebold, P. Blaha, L. Hammer, and G. S. Parkinson, Science **346**, 1215 (2014).